Available online at www.sciencedirect.com
SCIENCE DIRECT®
European Journal of Mechanics B/Fluids 25 (2006) 255–266

Free surface waves in equilibrium with a vortex

Alan R. Elcrat *, Kenneth G. Miller

Department of Mathematics, Wichita State University, Wichita, KS 67260, USA

Received 5 January 2005; received in revised form 14 September 2005; accepted 15 September 2005

Available online 25 October 2005

Abstract

Finite amplitude solitary waves of uniform depth which interact with a stationary point vortex are considered. Waves both with and without a submerged obstacle are computed. The method of solution is collocation of Bernoulli's equation at a finite number of points on the free surface coupled with equations for equilibrium of a point vortex. The stream function and vortex location are found by computing a conformal map of the flow domain to an infinite strip. For a given obstacle the solutions are parametrized with respect to Froude number and vortex circulation. When no obstacle is present there are two families of solutions, in one of which the amplitude of the wave increases by increasing the circulation, while in the other amplitude increases by decreasing the circulation. Beyond a certain critical Froude number the maximum amplitude wave has a sharp crest with an angle of 120 degrees. Similar behavior is observed for the flow past a submerged obstacle except that there is a critical Froude number below which there is no solution at all.

Keywords: Vortex; Solitary wave

1. Introduction

We are concerned with free surface flow in an infinite channel with gravity taken into account, in which there is embedded a point vortex stationary with respect to the flow. The fluid is inviscid and incompressible and the flow is irrotational except at the point vortex. Far upstream and downstream the flow is uniform with constant depth. The flows that we find are solitary waves with the same height and speed at infinity in both directions. We consider both flows over a flat bottom, which generalize the well-studied solitary waves of Russell and Stokes, [1–6] and flows past a submerged triangular obstacle which have been calculated by Dias and Vanden-Broeck [7] when there is no vortex.

The solution of this problem requires finding the location of a stationary vortex in a channel so that Bernoulli's equation is satisfied with constant pressure on the free surface. For any trial surface (i.e. a candidate for the free surface) the location of a stationary point vortex in equilibrium with the surface and the bottom of the channel is determined by using the Routh–Kirchhoff theory, [8,9], in conjunction with a conformal map between the flow domain and an infinite strip. This is done computationally by using the MATLAB package SCTOOLBOX of Driscoll [10]. Bernoulli's equation at a finite number of points on the free surface gives a system of equations which we then solve by Newton's method.

* Corresponding author.
E-mail address: elcrat@math.wichita.edu (A.R. Elcrat).

0997-7546/$ – see front matter
doi:10.1016/j.euromechflu.2005.09.001

For flow without an obstacle there are two dimensionless parameters, the Froude number and the dimensionless circulation k of the vortex. We solve for the free surface and the location of the vortex. For values of the Froude number F greater than one there is a solution for all $k,\ 0 < k \leqslant K_F$, where the maximal value depends on F. For at least a certain portion of this range there are two solutions, one a perturbation of the trivial uniform flow (with horizontal streamlines) for the given Froude number, and the other a generalization of the Russell solitary waves. The two families of solutions come together when $k = K_F$. Solutions in the first family are properly ordered with respect to amplitude in the sense that the amplitude of the wave increases with increasing k, while for the second family the amplitude of the wave decreases with increasing k. We recall that for the classic (no vortex) solitary wave of maximum amplitude, referred to as the Stokes wave, there is an angle of 120 degrees at the peak [2]. This wave has been studied extensively and its Froude number F_S has been computed by several different methods. (See [4,11,5] and references therein.) We have found that for $F > F_S$ there is a value of the circulation $k = \widetilde{K}_F < K_F$ for which the amplitude is maximal (among vortex solutions with the same Froude number) and this solution has a 120 degree angle at its peak. For $F \leqslant F_S$ the maximum amplitude occurs when $k = 0$ at the classic Russell solution for the given Froude number.

For flow past an obstacle we locate the position of a stationary vortex behind the obstacle. Although our computational method applies to any polygonal obstacle, in order to limit the number of parameters we have primarily restricted our attention to isosceles right triangles, as in Dias and Vanden-Broeck [7]. For a fixed (dimensionless) triangle height W the situation is similar to that described above for no obstacle except that there is a minimal Froude number > 1, depending on W, for which solutions exist, as found in [7]. The maximal circulation and the circulation of the maximum amplitude wave depend on W as well as F. We will refer to any solution with a 120 degree angle on the free surface as a Stokes solution, even if there is a vortex and/or an obstacle. There are three independent parameters for the full problem, $k,\ F$ and W and there is a two parameter family of Stokes solutions. The range of parameters for which solutions exist will be discussed in more detail below. It should be noted that for large Froude numbers, starting at about $F = 4.5$, the maximal solutions become very steep (nearly vertical) and for larger Froude numbers our method breaks down in attempting to reach either maximal circulation solutions or maximum amplitude solutions. At the end of Section 4 we consider, much more briefly, examples of flow past a semicircle and flow past a more general polygonal obstacle.

Free surface flows with vorticity have been studied previously in other contexts. The effects of a submerged point vortex moving with constant speed on a free surface have been investigated. See [12, p. 489] for a review of results obtained by linearization methods and Forbes [13] for a non-linear approach in the case of infinite depth. Free surface flows in which there is constant vorticity throughout the flow have been studied by Vanden-Broeck [14–16], Vanden-Broeck and Tuck [17], Vanden-Broeck and Kang [18], and McCue and Forbes [19].

2. Formulation of the problem

The flow domain is depicted in Fig. 1. (In some cases the obstacle is not present.) The flow domain D is bounded above by a free surface Γ, which is to be determined as part of the solution. At $\pm\infty$ the height of Γ is asymptotic to H and the velocity is U. If $v = v_1 + \mathrm{i}v_2$ is the velocity and ψ is the stream function, we can write $\bar{v} = 2\mathrm{i}\partial\psi/\partial z$ where $z = x + \mathrm{i}y$ and

$$\frac{\partial\psi}{\partial z} = \frac{1}{2}\left(\frac{\partial\psi}{\partial x} - \mathrm{i}\frac{\partial\psi}{\partial y}\right).$$

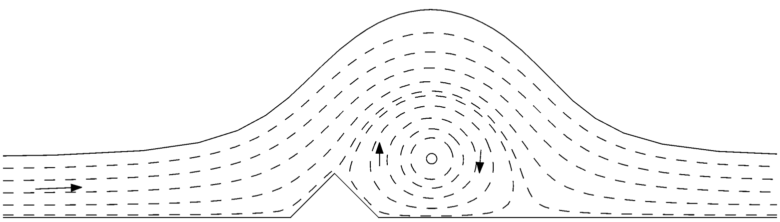

Fig. 1. A free surface wave in equilibrium with a vortex. The streamlines are dashed. The parameters for the flow shown are Froude number $F = 2.5$, circulation $k = 6.8$ and obstacle height $W = 0.4$.

We normalize ψ to be zero on the bottom; ψ is a positive constant on Γ which will be determined below. The nonlinear boundary condition on Γ is given by Bernoulli's equation. Assuming constant pressure on the free surface, this can be written as

$$|v|^2 + 2gy = U^2 + 2gH. \tag{1}$$

It is useful to introduce dimensionless variables. We use the normalization used by Dias and Vanden-Broeck [7],

$$V = v/(Qg)^{1/3}, \qquad Y = y/(Q^2/g)^{1/3}$$

where $Q = UH$ is the flow rate. Then

$$|V|^2 + 2Y = \widetilde{U}^2 + 2\widetilde{H}, \tag{2}$$

where

$$\widetilde{U} = U/(Qg)^{1/3}, \qquad \widetilde{H} = H/(Q^2/g)^{1/3}.$$

The Froude number is given by $F = U/\sqrt{gH} = \widetilde{U}/\sqrt{\widetilde{H}}$. Circulation k is made dimensionless by dividing by UH.

We assume that these dimensionless variables have been introduced and return to our original notation. We note that in these dimensionless variables

$$UH = 1, \qquad F = H^{-3/2}, \tag{3}$$

so Bernoulli's equation can be written

$$|v|^2 + 2y = H^{-2} + 2H. \tag{4}$$

Because of (3), for any given obstacle there are only two independent dimensionless parameters, the Froude number F (or equivalently the dimensionless height at infinity H), and the dimensionless circulation k of the vortex.

To determine the location of a stationary point vortex with circulation k in D, whether or not Bernoulli's equation is satisfied on Γ, we use the Routh–Kirchhoff theory, which we now discuss. We refer to [8] and [9] for general details of the theory and highlight those aspects that apply specifically to a channel-like domain D, for which a natural parameter domain is an infinite strip. The position of a single vortex in equilibrium with the boundary of D is at a critical point of the Kirchhoff–Routh path function W. W can be given explicitly in terms of a Green's function

$$g(z,w) = -\frac{1}{2\pi}\log|z-w| - h(z,w)$$

where g is constant on each component of ∂D and h is harmonic as a function of z. Let $R(z) = \frac{1}{2}h(z,z)$. Then

$$W(z) = k\eta(z) + k^2 R(z) \tag{5}$$

where η is the stream function for flow in D without a vortex. If $f : \widetilde{D} \to D$ is conformal, then

$$R(f(\zeta)) = \widetilde{R}(\zeta) - \frac{1}{4\pi}\log\left|f'(\zeta)\right| \tag{6}$$

where $\widetilde{R}$ is determined from the Green's function $\tilde{g}$ for $\widetilde{D}$ as above. If $\widetilde{D} = \{\zeta\colon\ 0 < \operatorname{Im}\zeta < H_o\}$, then $\tilde{g}$ can be computed explicitly by using the map $\zeta \mapsto w = \exp(\pi\zeta/H_o)$ from the strip to the upper half plane. Since

$$2\pi\tilde{g}(w_1,w_2) = -\log|w_1-w_2| + \log|w_1-\bar{w}_2|$$

we obtain

$$\widetilde{R}(\zeta) = -\frac{1}{4\pi}\log\left|\frac{\exp(\pi\zeta/H_o) - \exp(\pi\bar{\zeta}/H_o)}{(\pi/H_o)\exp(\pi\zeta/H_o)}\right| = -\frac{1}{8\pi}\log\left(\frac{2}{\pi^2}\bigl(1-\cos(2\pi\operatorname{Im}\zeta/H_o)\bigr)\right).$$

From (5) and (6) critical points of W are solutions of

$$\frac{\partial\tilde{\eta}}{\partial\zeta} + k\left(\frac{\partial\widetilde{R}}{\partial\zeta} - \frac{1}{8\pi}\frac{f''(\zeta)}{f'(\zeta)}\right) = 0 \tag{7}$$

where $\tilde{\eta}(\zeta) = c\,\mathrm{Im}\,\zeta$ is the stream function for potential flow in $\widetilde{D}$. To determine the value of c we assume that $f(\infty) = \infty$, which implies that $\mathrm{d}\zeta/\mathrm{d}z = H_o/H$ at infinity. The velocity is given by

$$\bar{v} = 2\mathrm{i}\frac{\partial\psi}{\partial z} = 2\mathrm{i}\frac{\partial\tilde{\psi}}{\partial\zeta}\frac{\mathrm{d}\zeta}{\mathrm{d}z} \tag{8}$$

with $\tilde{\psi}(\zeta) = c\,\mathrm{Im}\,\zeta - k\tilde{g}(\zeta,\zeta_o)$ and ζ_o the pre-image of the stationary point vortex (yet to be determined). Since $\partial\tilde{g}/\partial\zeta$ goes to 0 as ζ goes to ∞ in $\widetilde{D}$, $2\mathrm{i}\partial\tilde{\psi}/\partial\zeta$ goes to c. Hence $U = (H_o/H)c$ and by (3), $c = 1/H_o$.

The conformal map f we use is a Schwarz–Christoffel map determined numerically as discussed in the next section. For an infinite strip the Schwarz–Christoffel map is given by

$$f'(\zeta) = C\Pi\sinh\bigl(\pi(\zeta-\zeta_k)/2\bigr)^{\beta_k}$$

where $\pi(\beta_k+1)$ are the interior angles and ζ_k the preimages of the vertices of the polygonal domain. Therefore $f''(\zeta)/f'(\zeta)$ is a sum of terms of the form $\beta_k\coth(\pi(\zeta-\zeta_k)/2)\pi/2$, which can be computed readily since β_k and ζ_k are determined by the numerical conformal mapping routine.

After computing the conformal map to D we can find a stationary point vortex location by solving (7), either by Newton's method or some other numerical method. Once the location $z_o = f(\zeta_o)$ of a stationary vortex in D has been determined, the velocity on Γ can be computed from (8). We then vary Γ iteratively to satisfy Bernoulli's equation (4) as described in the next section.

3. Numerical implementation

We use a version of the Schwarz–Christoffel transformation to do the numerical conformal mapping part of our computation. Specifically we use the MATLAB package SCTOOLBOX developed by Driscoll [10] in which there is an option of using the infinite strip $\widetilde{D}_1 = \{\zeta\colon 0 < \mathrm{Im}\,\zeta < 1\}$ as the parameter domain. While the bottom of the flow domain D is polygonal, the free surface Γ is not. A mapping method which deals with smooth boundaries directly might be preferable, but software for this is not available in the public domain, and the convenience and reliability of SCTOOLBOX dictated our choice. One possibility is to use a polygonal approximation for Γ. However, an immediate problem with this approach is that at the pre-image of a corner $\mathrm{d}z/\mathrm{d}\zeta$ will be either 0 or undefined, and computing the velocity term in Bernoulli's equation by using (8) is problematic. We experimented with computing the velocity at points between the corners. However, we found that the following modification is preferable.

We use SCTOOLBOX to map $\widetilde{D}_1$ onto a polygonal domain with the base of D as the image of the real axis. We take Γ to be the image of the horizontal line $\mathrm{Im}\,\zeta = H_o$, $H_o < 1$. Γ is then an analytic curve. For $\delta > 0$, let $H_o = 1/(1+\delta)$. Then $H + \delta H$ is the height of the artificial polygonal channel at infinity. To define the polygonal strip in the physical domain one vertex far upstream and one vertex far downstream are fixed at height $H + \delta H$. The remaining n vertices on the upper boundary of the polygonal strip have fixed x-coordinates and varying y-coordinates which are the variables for our numerical algorithm. Pre-images of these n vertices are at points $\xi_j + \mathrm{i}$ on the upper boundary of $\widetilde{D}_1$. Images of the points $\xi_j + H_o\mathrm{i}$, $j = 1,\dots,n$, are then on Γ and Bernoulli's equation (4) at these points are the n equations which we solve numerically.

In cases where either there is no obstacle or where $k = 0$, there is a left-right symmetry to the problem, so we can cut the number of variables nearly in half by imposing this symmetry.

For flow past an obstacle, especially for large values of the circulation k, the significant features of the flow move further to the right of the obstacle and it is inconvenient to keep the x-coordinates of the vertices fixed. Therefore we have modified the procedure, keeping the relative distance between x-coordinates fixed but taking the x-coordinate x_m of the maximum point on Γ to be an additional variable. The equation added to the system is then an equation that imposes a horizontal tangent line at the point on Γ with x-coordinate x_m. This modification has the added advantage that the maximum point on the free surface is computed (whereas with the original method it could be between two vertices), allowing for more accurate calculation of the amplitude.

The above describes the method of discretization for all solutions except those of maximum amplitude, for which there is an angle of 120 degrees at the peak. Stokes' derivation that the maximum amplitude wave should have such a singularity, which can be found in [20] or [3], is equally valid when there is a vortex. To compute the singular solutions we have used a direct polygonal approximation, imposing Bernoulli's equation at points between the vertices. Since the peak vertex (x_m, y_m) is a stagnation point, Bernoulli's equation (4) implies

$$y_m = \frac{1}{2}H^{-2} + H \tag{9}$$

is determined. In the non-symmetric case we again take x_m as a variable with the relative distance between x-coordinates fixed. The two vertices adjacent to (x_m, y_m) are determined by imposing the 120 degree angle exactly. If n is the total number of vertices on Γ between the two vertices anchored at height H far up and downstream, this leaves $n-3$ heights to be determined along with x_m. For this problem, given H there is a solution for only one value k of the circulation. So k is included as a variable as well and we impose Bernoulli's equation at $n-1$ points between the vertices. We can alternatively keep k fixed and include H as a variable. We do this, in particular, to test the accuracy of our method when $k=0$ as discussed later.

For both the smooth case and the 120 degree angle case, we have solved the resulting system of equations using Newton's method with the partial derivatives in the Jacobian matrix approximated by first order forward differences. The value of δ was typically set at 0.02 and the difference increment in the forward differences was taken to be 10^{-7}. Newton's method was continued until equations were solved to machine precision. The anchored points far upstream and downstream have been typically placed at $x = \pm 7$. Moving them further toward infinity did not make a discernable effect on the solution.

A good initial guess is required for this procedure to work. Solutions were first obtained near the limiting case of no obstacle and no vortex. For the maximum amplitude wave an initial guess of the form

$$y = H + \frac{1}{2}H^{-2}\exp\bigl(-\lambda|x|\bigr)$$

proved useful. The 120 degree angle fixes λ, $\lambda = 2H^2/\sqrt{3}$, and the value of $H = 0.843$ computed in [11] gives a starting foothold when there is no vortex and no obstacle. Continuation from previously obtained solutions by small increments of the parameters F, k and the height W of the triangle was used to obtain the solutions described below. Rough solutions can be obtained using relatively few discretization points and then refinements made using interpolation to initialize with more points.

4. Results

We give results for (a) no obstacle, (b) triangular obstacles, (c) a semicircular obstacle, and (d) a representative more general polygonal obstacle. We have carried out an investigation of the parameter range for which solutions exist in the first two cases.

4.1. No obstacle

When there is no obstacle, a solution can be viewed as a traveling solitary wave with a vortex moving in equilibrium with the wave. In dimensionless variables the wave speed $U = 1/H$, where the height H at infinity is determined by the Froude number according to (3). A typical flow is shown in Fig. 2.

Fig. 3 shows the range of the parameters k and F for which solutions have been found. As discussed in the Introduction, there are two families of solutions. Two representative sequences of wave profiles with fixed F and varying k are given in Figs. 4 and 5. In the first case $F \leqslant F_S$, the Froude number of the classic Stokes wave, and there

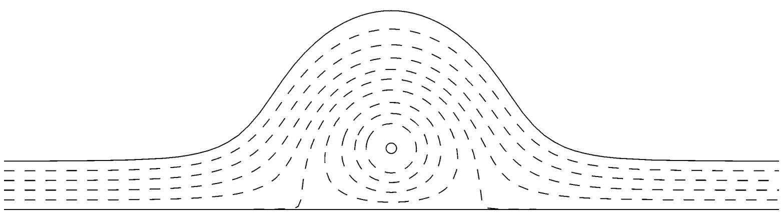

Fig. 2. A flow with $F = 2.828$ ($H = 0.5$) and $k = 8.77$. Streamlines are dashed.

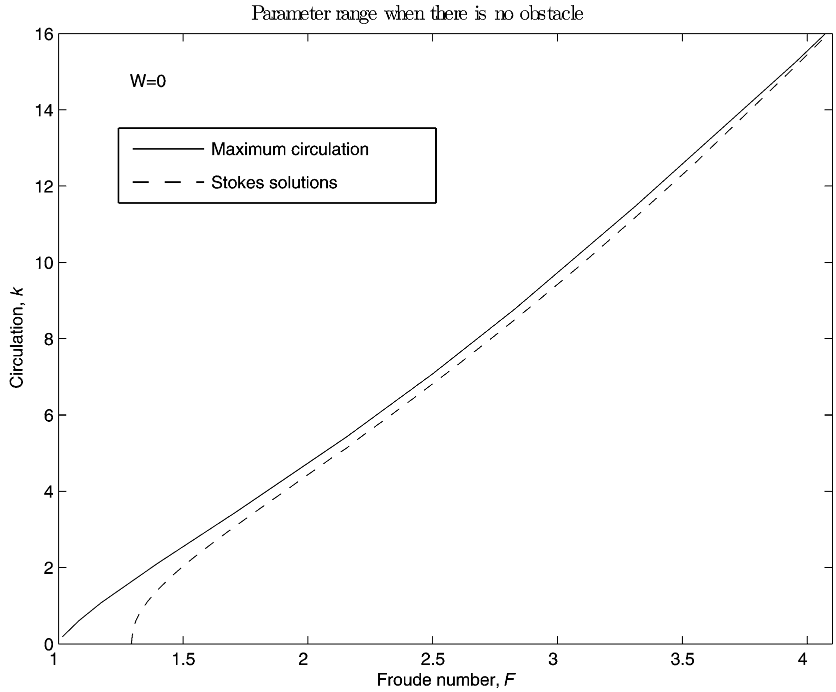

Fig. 3. Range of the parameters k and F for which there are solutions when $W = 0$. The solid curve gives the maximal circulation K_F for which there is a solution with Froude number F. Between the two curves there are two solutions; below the dashed curve only one. For parameters on the dashed curve there is a maximum amplitude solution with a 120 degree angle singularity. The dashed curve meets the axis at $F_S = 1.291$, the Froude number of the classic Stokes wave.

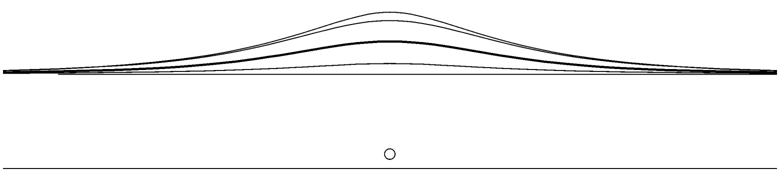

Fig. 4. A sequence of wave profiles when $F = 1.276$ ($H = 0.85$). From bottom to top the values of k are 0, 1, $K_F = 1.57$, 1 and 0 (the Russell wave). The location of the point vortex with maximum circulation is indicated. The vertical segment from this point to the base is the locus of possible vortex locations.

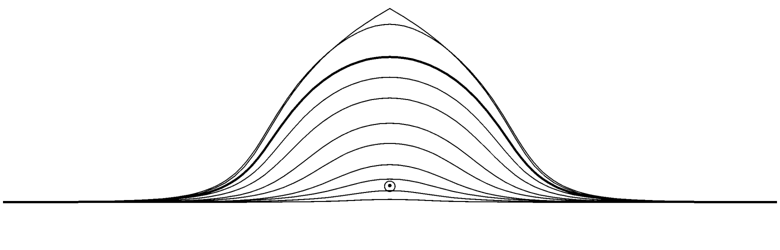

Fig. 5. A sequence of wave profiles when $F = 2.828$ ($H = 0.5$). The solution with maximum circulation $K_F = 8.77$ is highlighted. The circulation of the Stokes solution is $\widetilde{K}_F = 8.50$. The location of the point vortex with maximum circulation is indicated.

are two solutions for all k, $0 < k \leqslant K_F$. In the second case F is considerably larger than F_S and the upper family of solutions exists for only a small range of k.

It is apparent from Fig. 4 that variations in amplitude are not uniform with respect to variations in k. Fig. 6 shows the relative amplitude τ of the free surfaces versus k for the two values of F considered in Figs. 4 and 5 as well as

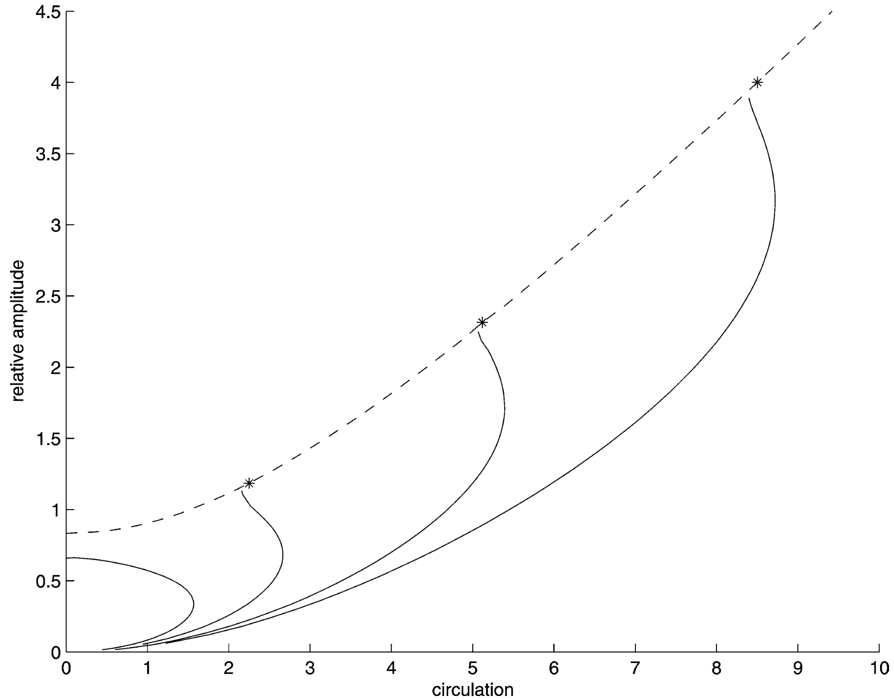

Fig. 6. Relative amplitude τ versus k. The Froude number F is constant on each solid curve. Values of F from left to right are 1.276, 1.540, 2.152 and 2.828. The dashed curve gives the relative amplitude of the Stokes solutions as a function of k, with *'s indicating the Stokes solution for the given values of F. The position of the terminal point on the computed solid curves relative to the * for the corresponding Stokes solution indicates that among flows with a fixed vortex circulation, there is a solution with amplitude slightly less than that of the Stokes solution, but with a greater Froude number. For free-surface flows without vortex this phenomenon was observed by Longuet-Higgins and Fenton [5].

for two other values of F. If the amplitude a is defined as the vertical distance from the maximum point on Γ to the horizontal axis, then τ is defined by

$$\tau = \frac{a}{H} - 1$$

where H, the height at infinity, is constant for constant F by (3). For any F, in the lower family of solutions the amplitude of the wave increases with increasing k, while in the upper family the amplitude of the wave decreases with increasing k.

We have found that the family of upper solutions can be continued from the solid curve to just below the dashed curve in Fig. 3. This indicates that among the upper solutions with k fixed, the Stokes wave does not have the maximum Froude number, or velocity at infinity, as can also be seen in Fig. 6. This aspect of the behavior of solitary waves when there is no vortex is discussed in [5] and [4]. Although we have found this observation to hold consistently when doing continuations, it should be noted that the difference in the Froude numbers between the maximum amplitude solution (Stokes solution) and the maximum velocity solution (maximal among upper solutions with k fixed) is of roughly the same magnitude as the expected accuracy of our solutions. There should apparently be a very small third family of solutions (assuming continuity of the family of solutions with respect to the parameters when approaching the Stokes solutions), however we have not been able to conclusively distinguish solutions in such a third family.

Fig. 6 indicates that in determining solutions with nearly maximal circulation by continuation from nearby solutions, k is not an appropriate parameter. We were not able to continue from the lower family of solutions through the maximum circulation solution to the upper family using k as the continuation parameter. However, we can use a variation of our usual routine whereby we fix the amplitude a and consider k as one of the variables. The amplitude is a satisfactory continuation parameter for going between the upper and lower families.

4.2. Triangular obstacles

When the triangular obstacle is present we have found stationary vortices both directly above the obstacle and behind the obstacle, but consider only the latter in our discussion. For those above the obstacle the results are similar but the range of possible circulation values is smaller for given F and obstacle height W. When there is no vortex, flows were computed in [7]. For any given W there is a Froude number $F_W > 1$ below which there is no flow, the value of F_W increasing as the height W of the triangle increases. The results we obtain when there is an obstacle are very similar to those given above for a flat channel floor except that the parameter range shrinks as W increases. Fig. 7 shows the parameter range for $W = 0.4$, and Figs. 8 and 9 give sequences of wave profiles similar to those presented when there is no obstacle.

For a fixed Froude number there is a maximum triangle height W for which solutions exist. Fig. 10 shows the range of the parameters k and W for which solutions exist when $F = 2.1517$ ($H = 0.6$). As the maximum value of W is approached the maximum circulation decreases rapidly. Fig. 11 shows streamline plots of the maximal circulation flows at this Froude number for various triangles. The amplitudes of the free surfaces in Fig. 11 are nearly identical. The shapes of the waves vary somewhat, depending on the relative sizes of the obstacle and vortex. It is noted that the Stokes waves with fixed F all have the same amplitude by (9).

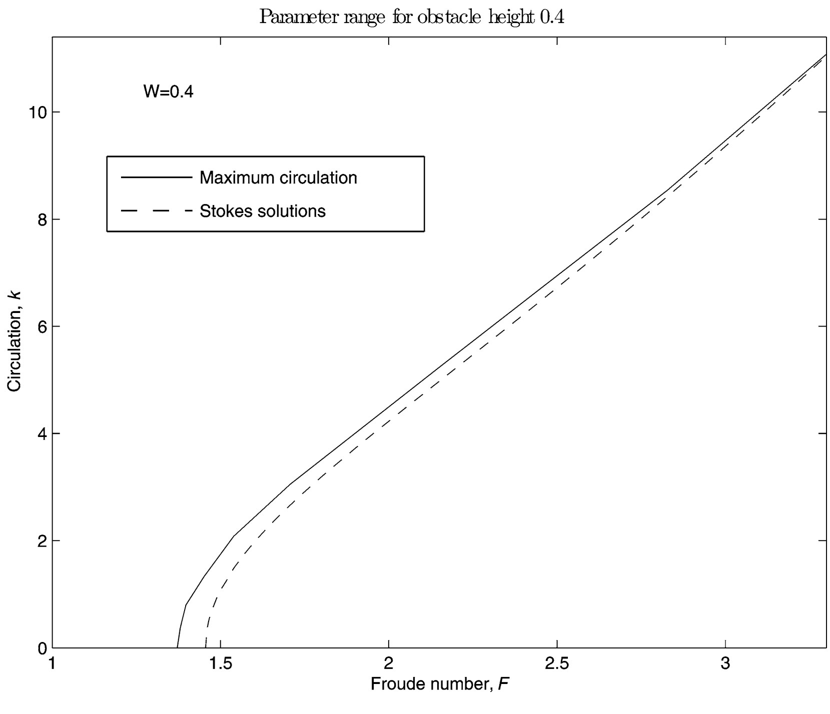

Fig. 7. For $W = 0.4$ there are no solutions for $F < 1.372$. There is a Stokes solutions for each $F \geqslant 1.456$. Between the two curves there is both an upper and lower solution. The curves in this figure asymptotically approach their counterparts in Fig. 3.

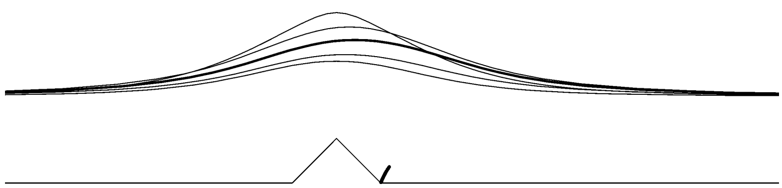

Fig. 8. A sequence of wave profiles when $F = 1.45$ and $W = 0.4$. The solution with maximum circulation $K_F = 1.335$ is highlighted. The maximum amplitude solution is smooth at its peak. This Froude number is slightly less than the value where Stokes solutions exist. The entire locus of point vortex locations for this F is shown.

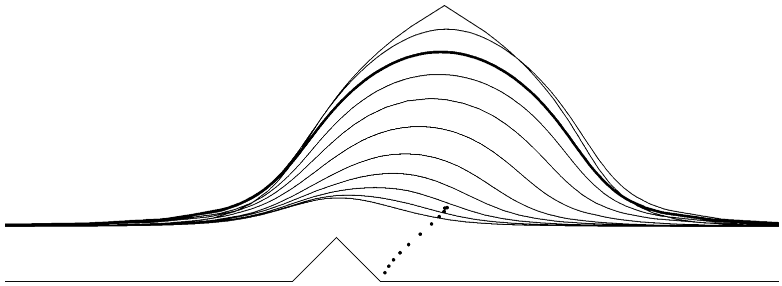

Fig. 9. A sequence of wave profiles when $F = 2.828$ and $W = 0.4$. Circulations for the waves shown are $1.2, 2.4, 3.6, 4.8, 6.0, 7.2, 8.1, 8.5, 8.58$ (maximum circulation), 8.5 and 8.43 (the Stokes solution.) Ordinates of the vortex locations increase with amplitude. Likewise for the abscissa, except the abscissa for the Stokes solution is 0.018 units to the left of that for the next highest solution. (The vortex locations for these two highest amplitude solutions are not clearly distinguishable on the graph.)

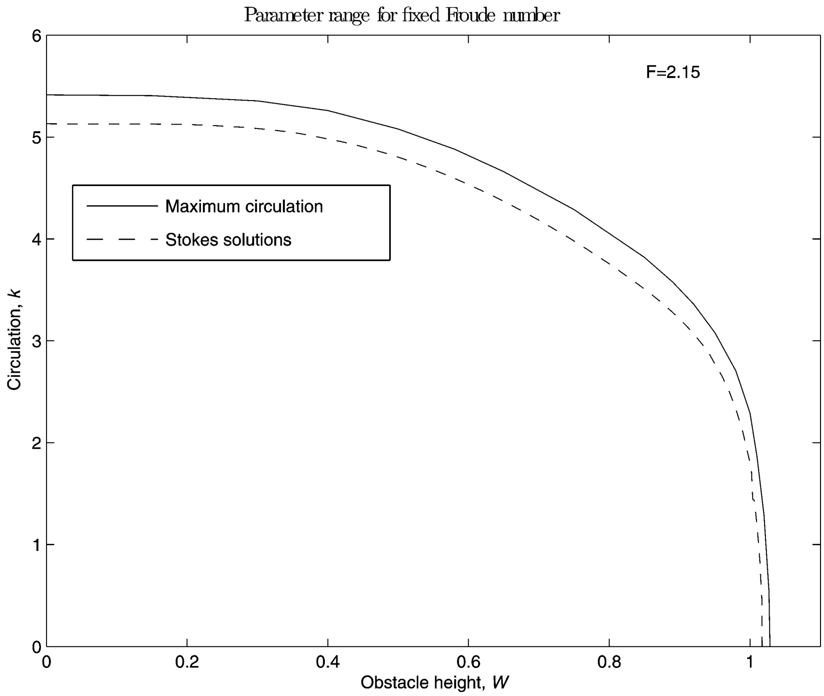

Fig. 10. With $H = 0.6$ ($F = 2.1517$) there are no solutions for $W > 1.0284$. There is no Stokes solution for $W > 1.0173$. Between the two curves there is both an upper and a lower solution.

All of the free surface waves presented so far have a single peak. However, that is not necessarily the case, as Fig. 12 shows. The Froude number is quite large in this example and the circulation is far from maximal. All solutions we have found that are near maximal have a more standard solitary wave profile. As noted in the introduction, for Froude numbers above about 4.5 the maximal solutions become extremely steep. Fig. 13 shows one computed example.

4.3. Semicircular obstacle

To compute solutions when there is a semicircular obstacle, we have made use of the Joukowski transformation $J(w) = w + r^2/w$ which maps the exterior of a semicircle of radius r in the upper half plane onto the entire upper half plane. The conformal map is then $f = J^{-1} \circ f_1$ where f_1 is a Schwarz–Christoffel map as before where the image base is the entire real axis. Except for the necessary modification to $f''(\zeta)/f'(\zeta)$ in Eq. (7), all details of the numerical method are the same as before. Fig. 14 shows a sequence of wave profiles for flow past a semicircle of radius 0.4 and a streamline plot for the maximum circulation flow is given in Fig. 15.

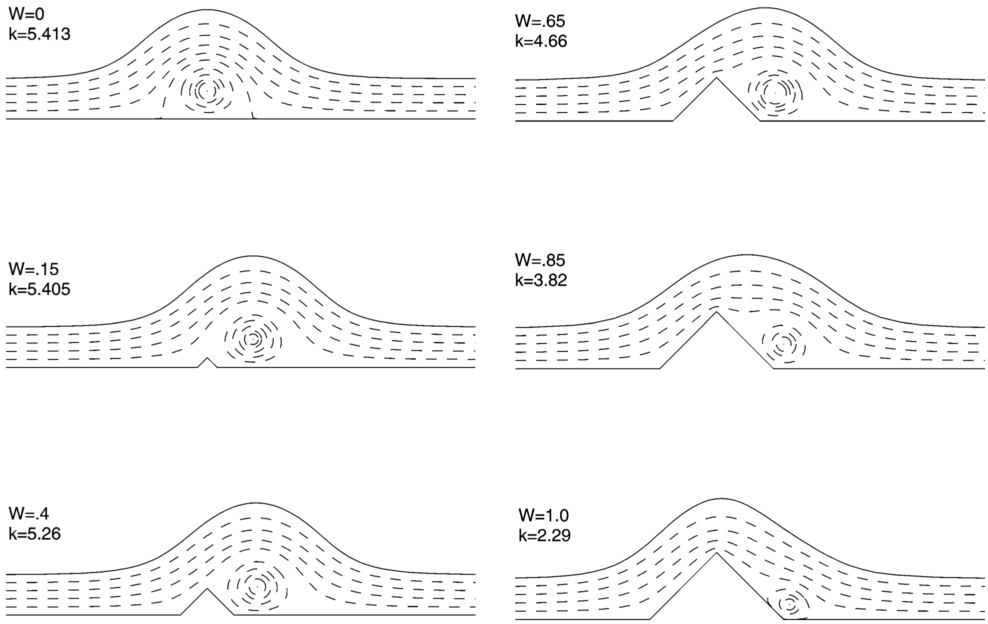

Fig. 11. Maximum circulation flows for fixed Froude number, various obstacle heights. The value of F is 2.1517 ($H = 0.6$).

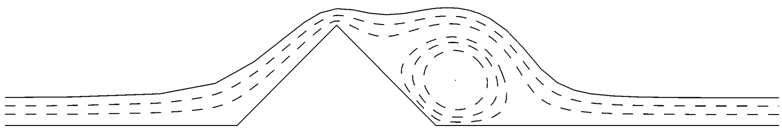

Fig. 12. A free surface with two maxima. The parameters are $F = 8$, $W = 0.9$ and $k = 12.4$.

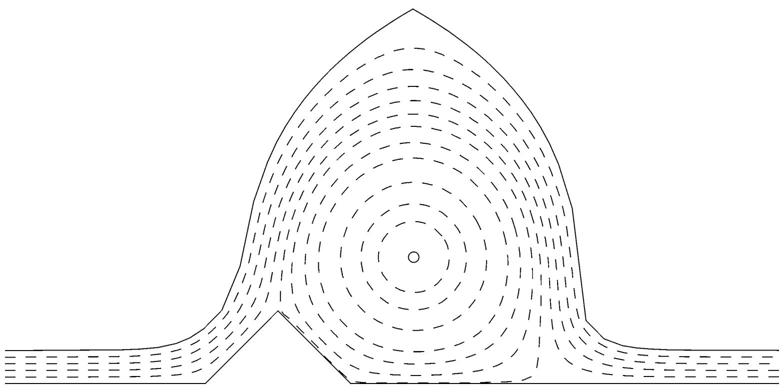

Fig. 13. The maximum amplitude flow with $F = 4.54$, $W = 0.8$, $k = 18.8$.

4.4. Other polygonal obstacles

Our method using SCTOOLBOX works for general polygonal obstacles. For such obstacles there may be several families of vortices, depending on the shape of the obstacle. For the step-shaped obstacle shown in Fig. 16 there are four families of vortices for a given Froude number. Each of these families can be continued to a distinct Stokes solution. The maximum circulation for each of the families is different, however the amplitudes of these maximum circulation solutions are nearly the same, as can be seen in Fig. 16. As noted earlier, the amplitude of the Stokes solutions depends only of the Froude number.

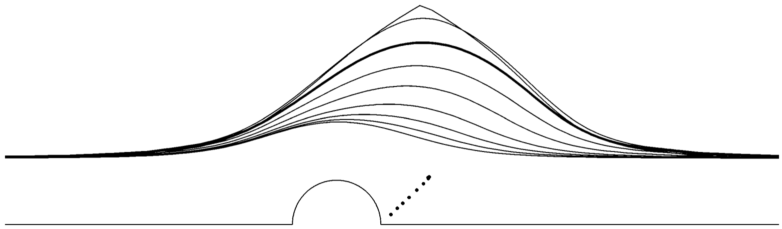

Fig. 14. A sequence of wave profiles for flow past a semicircle of radius $r = 0.4$ when $H = 0.6$ ($F = 2.1517$). Circulations for the waves shown are $1.0, 2.0, 2.8, 3.6, 4.4, 4.9, 5.09$ (maximum circulation), 4.9 and 4.84 (the Stokes solution). The vortex locations for the three highest amplitude solutions are not clearly distinguishable on the graph.

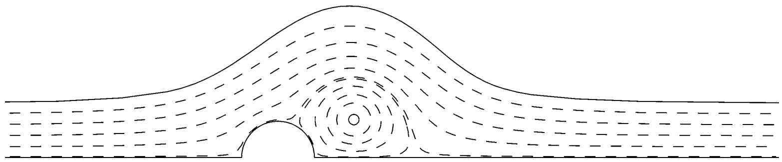

Fig. 15. Streamline plot for the maximum circulation solution for flow past a semicircle of radius $r = 0.4$ with $F = 2.1517$.

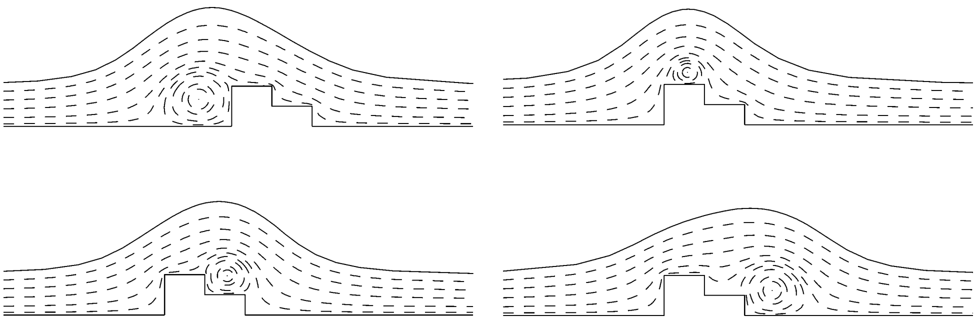

Fig. 16. There are four families of vortices for flow past this obstacle. The width of the obstacle is 1.2 and the height is 0.6. The value of F is 2.1517, the same as in Fig. 11. The maximum circulation solution for each of the four families is shown. The respective maximum circulation values are $k = 4.5$, $k = 3.0$, $k = 3.81$, and $k = 4.28$.

5. Accuracy

Previously computed values of the Froude number for the classic Stokes wave provide a benchmark to measure the accuracy of our method. For waves with a 120 degree singularity, our solution method depends on the location of the points between the vertices where Bernoulli's equation is imposed. Depending on the choice of those points, with $n = 24$ (here n is the number of variables for a symmetric problem so there are $2n - 1$ vertices on the upper polygonal free surface) our determination of F varies by $\pm 1\%$ from the value of 1.2909 given in [11]. With $n = 45$ this improves to a maximum deviation of $\pm 0.5\%$. The best value, in which the error is less than $\pm 0.1\%$, happened to be obtained by positioning points for evaluating Bernoulli's equation at the golden mean between the midpoint of an edge and one of the vertices. We have used this positioning in our computations of other Stokes waves.

For any values of the parameters F, k and W, we can check the consistency of the computations as n is increased. (We now consider the non-symmetric case, and the number of variables equals the number of vertices on the upper channel.) We compare the computed values of the amplitude a between solutions obtained with different n. For illustration, we consider two cases in both of which $F = 2.15$. The first, which can be considered typical, has $k = 4$. The second is more difficult in that the solution is near the maximal circulation $k = 5.22$ and the free surface is steeper. In the first case the difference between the value of a with $n = 33$ and the value with $n = 53$ is less than 0.5%; with $n = 43$ and $n = 53$ the difference is less than 0.2%. In the second case the difference between the value with $n = 33$ and the value with $n = 57$ is about 10%; with $n = 51$ and $n = 57$ the difference is about 1%. The number of points needed for a certain level of accuracy becomes greater as the free surfaces become steeper. For some of the larger amplitude solutions errors in the 2 to 3 percent range would not be unexpected.

6. Conclusions

We have computed solitary waves in water of finite depth, with and without an obstacle on the bottom, when a point vortex is in equilibrium with the flow. In the case of triangular obstacles we have done a parametric study relating the Froude number, vortex circulation and the obstacle height. The flows have been computed in the physical plane using a conformal mapping method for solving the related potential flow problem. The conformal map has been obtained using a variant of the Schwarz–Christoffel transformation implemented using Driscoll's SCTOOLBOX. The flows have been obtained up to a maximum amplitude for the wave where there is a stagnation point with a 120 degree angle at the peak. The flows we have studied are a first step in a program of finding equilibrium free surface flows with vorticity. For flows with constant vorticity throughout the flow this has been studied in [14–18], and [19]. We plan to use the point vortex flows found here as starting points for finding vortex patches in free surface flows as in [21].

References

[1] J.S. Russell, Report on waves, Rep. 14th Meeting Brit. Assn. Adv. Sci., York, 1844, John Murray, London, 1845, pp. 311–390.
[2] G.G. Stokes, On the theory of oscillatory waves, in: G.G. Stokes, Mathematical and Physical Papers, vol. 1, Cambridge Univ. Press, Cambridge, 1880, pp. 197–229, 314.
[3] C.J. Amick, L.E. Fraenkel, J.F. Toland, On the Stokes conjecture for the wave of extreme form, Acta Math. 148 (1982) 193–214.
[4] J.G.B. Byatt-Smith, M.S. Longuet-Higgins, On the speed and profile of steep solitary waves, Proc. Roy. Soc. London Ser. A 350 (1976) 175–189.
[5] M.S. Longuet-Higgins, J.D. Fenton, On the mass, momentum, energy and circulation of a solitary wave, II, Proc. Roy. Soc. London Ser. A 340 (1974) 471–493.
[6] J.W. Miles, Solitary waves, Ann. Rev. Fluid Mech. 12 (1980) 11–43.
[7] F. Dias, J.-M. Vanden-Broeck, Open channel flows with submerged obstructions, J. Fluid Mech. 206 (1989) 155–170.
[8] P.G. Saffman, Vortex Dynamics, Cambridge University Press, Cambridge, 1992.
[9] C.C. Lin, On the Motion of Vortices in Two Dimensions, Univ. Toronto Appl. Math. Ser., vol. 5, Toronto Univ. Press, Toronto, 1943.
[10] T.A. Driscoll, A MATLAB Toolbox for Schwarz–Christoffel mapping, ACM Trans. Math. Soft. 22 (1996) 168–186.
[11] J.K. Hunter, J.-M. Vanden-Broeck, Accurate computations for steep solitary waves, J. Fluid Mech. 136 (1983) 63–71.
[12] J.V. Wehausen, E.V. Laitone, Surface Waves, Handbuch der Physik, vol. 9, Springer-Verlag, Berlin, 1960.
[13] L.K. Forbes, On the effects of nonlinearity in free-surface flow about a submerged point vortex, J. Engrg. Math. 19 (1985) 139–155.
[14] J.-M. Vanden-Broeck, Steep solitary waves in water of finite depth with constant vorticity, J. Fluid Mech. 274 (1994) 339–348.
[15] J.-M. Vanden-Broeck, New families of steep solitary waves in water of finite depth with constant vorticity, Eur. J. Mech. B Fluids 14 (1995) 761–774.
[16] J.-M. Vanden-Broeck, Periodic waves with constant vorticity in water of finite depth, IMA J. Appl. Math. 56 (1996) 207–217.
[17] J.-M. Vanden-Broeck, E.O. Tuck, Steady inviscid rotational flows with free surfaces, J. Fluid Mech. 258 (1994) 105–113.
[18] J.-M. Vanden-Broeck, Y. Kang, Gravity-capillary waves in the presence of constant vorticity, Eur. J. Mech. B Fluids 19 (2000) 253–268.
[19] S.W. McCue, L.K. Forbes, Bow and stern flows with constant vorticity, J. Fluid Mech. 399 (1999) 277–300.
[20] R.S. Johnson, Modern Introduction to the Mathematical Theory of Water Waves, Cambridge Univ. Press, Cambridge, 1997.
[21] A. Elcrat, B. Fornberg, M. Horn, K. Miller, Some steady vortex flows past a circular cylinder, J. Fluid Mech. 409 (2000) 13–27.